2020 Mediterranean and Middle-East Geoscience and Remote Sensing Symposium (M2GARSS), 9-11 March 2020
Tunis, Tunisia, pp. 25-28
DOI: 10.1109/M2GARSS47143.2020.9105296

PHYSICS-BASED CLUTTER MODEL FOR GEOSYNCHRONOUS SYNTHETIC APERTURE RADAR

C. Convenevole, S.E. Hobbs

Space Research Group
School of Aerospace, Transport and Manufacturing
Cranfield University, College Road, MK43 0AL, UK

ABSTRACT

In this paper the land clutter literature is briefly discussed and a need for a new class of clutter models for the Geosynchronous Synthetic Aperture Radar System Performance Assessment is shown. A new physics-based clutter model that uses data on observed vegetation motion is introduced and a wheat database is presented together with an analysis of the plant motion statistics. After this, the characteristics of the new model are outlined. Then the analysis of the wheat signal is developed for all the available data, and subsequently the properties of the moving target signal are related to a more ideal plant motion.

Finally, the obtained model for the target coherent power is illustrated together with the future work needed to complete the clutter model. This approach, developed for the Geosynchronous Synthetic Aperture Radar performance estimation, promises a versatile model suitable for a wide range of SAR systems.

Index Terms— GEO SAR clutter, Parametric land clutter model, SAR clutter, wheat clutter model

1. INTRODUCTION

Geosynchronous Synthetic Aperture Radar (GEO SAR) has attracted increasing interest in the last two decades. The concept is now widely accepted, but there are some concerns on the performance achievable on non-static target scenes. The movement of a target in a SAR system causes target signal to be smeared in the azimuth direction. This smeared signal is a form of clutter. For some GEO SAR mission concepts, the azimuth spread of the power scattered from clutter is a potentially important constraint on imaging performance because it smears a noise-like power across the image. Models of GEO SAR imaging therefore need to include clutter spread [1, 2].

A well-known and widely accepted radar land clutter model is Billingsley's Intrinsic Clutter Model [3, 4, 5]. This was developed for radar imaging of vegetation with a depression angle of $5°$ - $10°$ (incidence $80°$ - $85°$, typical for airborne radar). The geometry of geosynchronous orbit (GEO) satellite radar is quite different with incidence angles of $20°$ - $70°$. For spaceborne radar we expect less shadowing of clutter patches and more scatter from within the canopy. Billingsley's work does however include models of the relationship between windspeed and clutter scattering. This is useful for GEO SAR because for some systems the proposed relative orbit speed is relatively low, which combined with the long slant range can lead to very large azimuth spread of clutter backscatter.

We propose a novel physics-based approach which promises to provide a generic approach to clutter modelling suitable for a wide range of incidence angles and wavelengths. It is based on observations of the true motion of vegetation (wheat, in the first case) in natural wind. These are combined with a focussing algorithm to assess how broadly the scattered power is smeared in azimuth across the image. Parametrisations of the azimuth spread for a particular class of vegetation (wheat, representing short crops) are derived to allow image simulation for a range of landscapes and weather conditions. We expect that similar parametrisation could be developed for other landcover classes, for example rough water, long crops and trees / forest (probably the most important class needed to represent real landscapes).

In section 2 the paper presents the plant motion database; section 3 contains a set of motion and clutter spread parametrisations; finally, section 4 presents our baseline wheat clutter model. The paper closes with a brief discussion and some conclusions.

2. WHEAT MOVEMENT DATABASE

A previous experiment (June to August 2000) has been conducted using stereo imaging to measure vegetation movement in wind [6]. A database of wheat movement and wind velocity at 10 m height has been collected [7].

The crop top position of a variable number of wheat plants has been recorded at a frequency of 25 Hz. A target quality flag tells if the target is visible or not and this latter case is defined as a gap in the time series.

In the database the X reference axis is aligned with the

wind mean direction, so different azimuth directions (ψ) relative to the slant range allow to simulate different wind directions. The slant range direction is defined by incidence angle (θ) and ψ.

3. WHEAT MOVEMENT ANALYSIS

The wheat movement is driven by the wind and due to its turbulent nature it is quite difficult to model the movement of a single wheat plant. Thus we decided to analyse the statistics of the available targets assuming that they are representative of the whole wheat field.

The statistical properties that have been analysed are: mean velocity, standard deviation of the velocity and standard deviation of displacement from mean position. They are all computed in the slant range direction, that we omit to say every time for brevity.

3.1. Analysis of wheat velocity

Due to the uncertainty of the data, the wheat velocity has been computed with a linear regression on an interval of 0.20 s and the value of velocity is considered only if the plant is visible during the whole interval.

The wheat mean velocity is zero because the wheat has no net displacement. The distribution of the instantaneous wheat velocity, shown in Fig. 1a, has been studied and compared with the distribution of the signal simulated with the wheat data, shown in Fig. 1b. Since the two distributions have a different shape, we concluded that the velocity distribution is not sufficient to estimate the distribution of clutter power.

3.2. Analysis of wheat displacement standard deviation

The displacement standard deviation of each day's data has been computed for different incidence and azimuth that represent different geometries of the system (e.g. Fig. 2).

Windspeed differs from day to day, so using all the available data we can plot the position standard deviation against the windspeed. In Fig. 3 we can see this plot for $20° \leq \theta \leq 70°$ and $0° \leq \psi \leq 360°$. To model this, two straight lines are used, as shown, with a change in slope at just over 5 m/s.

3.3. Loss of power due to visibility gaps

A single range gate monostatic SAR simulator has been developed to simulate the signal of the aforementioned wheat movement database; the focusing algorithm of this simulator is the backprojection algorithm.

The presence of gaps in the visibility of the target leads to a loss of power in the image, compared to the transmitted power (P_t), because the simulator does not collect any echo if the target is not visible.

A correlation has been found among the received power (P_r), the number of pulses in which the target is visible (n_{vp}),

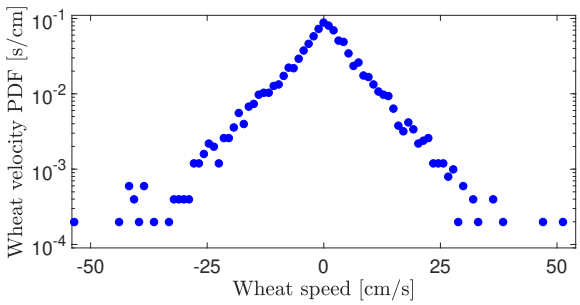

(a) PDF of the velocity in slant range direction.

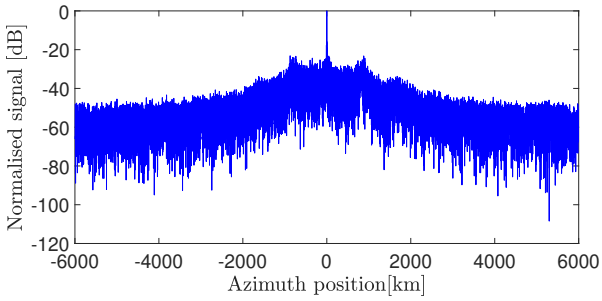

(b) Normalised focused image.

Fig. 1: 2^{nd} of August, mean windspeed = 2.54 m/s, $v_y = 5$ m/s, $\lambda = 40$ cm, $\theta = 65°$, $\psi = 0°$.

the total number of pulses (n_p) and P_t; this correlation is shown in Eq. 1 and its validation, that allows a power normalisation even with the gaps in the data, is shown in Fig. 4 where we have the plot of the ratio between the simulated image power (P_{sim}) and P_r.

$$P_r \propto P_t \cdot \frac{n_{vp}}{n_p} \tag{1}$$

4. WHEAT CLUTTER MODEL

The performance methodology [1] requires the knowledge of the clutter power distribution; this distribution is the probab-

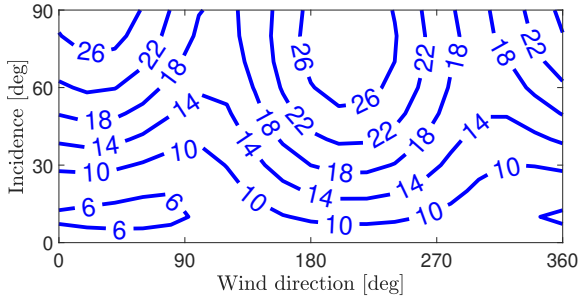

Fig. 2: 2^{nd} of August, wheat displacement standard deviation in mm along the slant range direction. Windspeed = 6.6 m/s.

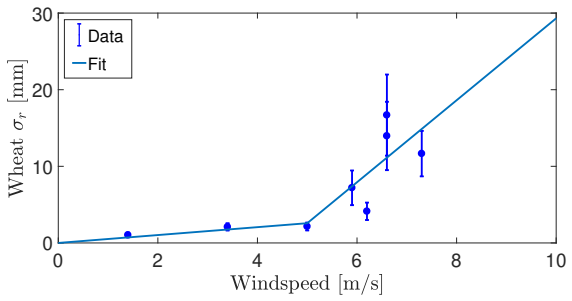

Fig. 3: Wheat displacement standard deviation ($20° \leq \theta \leq 70°$ and $0° \leq \psi \leq 360°$) as function of the windspeed extrapolated to 10 m height.

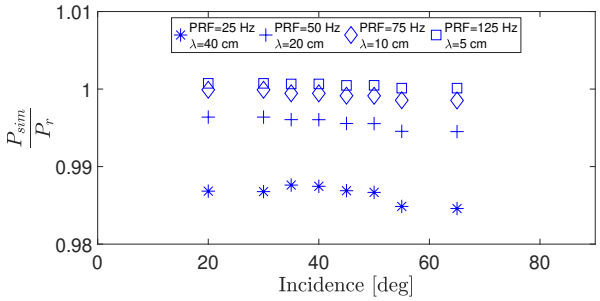

Fig. 4: $\frac{P_{sim}}{P_r}$, difference from 1 are assumed to be due to (a) power outside the integration domain (b) numerical rounding, 2^{nd} of August, $\psi = 0°$, $v_y = 10$ m/s.

ility density function (PDF) of the power backscattered from the moving target. Knowing the PDF means that we know its shape and spread distance for the given simulation parameters. Those parameters are: the season (ς), landcover (Λ), windspeed (W), wavelength (λ), azimuth speed (v_y), θ and ψ. We can express the PDF function dependency as the following equation:

$$PDF = f(y, \varsigma, \Lambda, W, \lambda, v_y, \theta, \psi) \tag{2}$$

Because it would be very difficult to know the wind direction relative to the slant range and because of the variability of the wheat displacement standard deviation distribution (e.g. Fig. 2), we can say that a model like Eq. 2 is practically impossible to be applied and so we have to approximate our model and reduce the parameters we consider. Thus we get the following relation (that is built averaging on the wind direction):

$$PDF = f(y, \varsigma, \Lambda, W, \lambda, v_y, \theta) \tag{3}$$

4.1. Coherent and incoherent power fraction definition

Like in the Billingsley model [5], we divided the target power in two components: one appears in the target nominal position (we call it signal power, P^{sig}) and the rest is spread in the azimuth direction (we call it clutter power, P^{cl}). They are defined as follows:

$$P_r = P^{sig} + P^{cl} \tag{4}$$

$$\Gamma = \frac{P^{sig}}{P_r} \tag{5}$$

$$\Omega = \frac{P^{cl}}{P_r} \tag{6}$$

$$\Gamma = \int_{-\rho_y}^{\rho_y} \gamma(y)\, dy \tag{7}$$

$$\Omega = \int_{-\infty}^{-\rho_y} \omega(y)\, dy + \int_{\rho_y}^{+\infty} \omega(y)\, dy \tag{8}$$

$$PDF(y) = \begin{cases} \gamma(y), & \text{for } |y| \leq \rho_y \\ \omega(y), & \text{for } |y| > \rho_y \end{cases} \tag{9}$$

where we have the coherent power fraction (Γ), the incoherent power fraction (Ω) and the azimuth resolution (ρ_y).

4.2. Coherent power estimation and modelling

For each day, different geometry conditions give a different power in the central peak and this has been related to the target phase uncertainty (σ_ϕ); this is shown in Fig. 5. σ_ϕ is computed from the displacement standard deviation (σ_r), with the following equation:

$$\sigma_\phi = \frac{4\pi}{\lambda} \cdot \sigma_r \tag{10}$$

Although the received power could be computed using Eq. 1, the target is decorrelated by the gaps and thus the Γ is lower than in the case of having the same σ_ϕ but a continuous visibility of the target. However, there is a clear trend in all the eight days and a bell shape curve has been proposed to model the target coherent power. This modelling curve is very close to the coherent power distribution of a normal random distributed target with no gaps (the scattered points in Fig. 5); moreover, we assume that in a real case, if something is hidden, it means that there is something in front of it that is hiding it. Under this assumption, we can replace the real wheat motion with a simulated motion having the same standard deviation but having no gaps. This gives us the curve in Fig. 5 (solid line) that has the expression of Eq. 11,

$$\Gamma = \Gamma_0 \cdot \exp\left(-\left(\frac{\sigma_\phi}{\sigma_0}\right)^2\right) \tag{11}$$

where we have the standard deviation of the target phase (σ_ϕ) defined by Eq. 10. The values of the two parameters (Γ_0 and σ_0) are summarised in Tab. 1. With this model, even for a static target there are side-lobes which push some power into the tails (because the signal of the static target does not appear only in the target position).

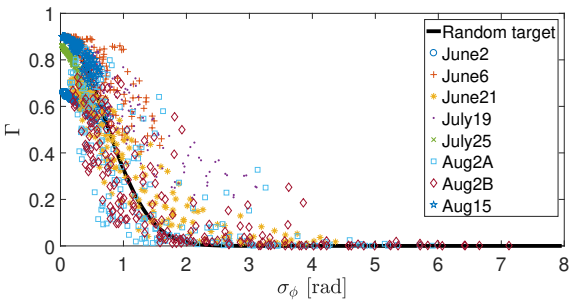

Fig. 5: Coherent power related to the σ_ϕ, $\lambda = 10$ cm, $v_y = 10$ m/s, $20° < \theta < 70°$, $0° \leq \psi < 360°$. Scattered points are the wheat data, the line is the random phase target.

Table 1: Fit of wheat data and of the random target

	Γ_0	$\sigma_0\ [rad]$
Real data	0.80525 ± 0.01160	1.3301 ± 0.0345
Random target	0.9096 ± 0.0001	0.9985 ± 0.0001

4.3. Numerical results

We made a least square fit with a Gaussian function for the data shown in Fig. 5 and the results is compared to the fit of the random target signal in Tab. 1. One of the possible explanation for the difference between the two fit functions is the loss of coherence caused by the gaps in the data.

5. CONCLUSIONS AND FUTURE WORK

The objective of this paper was to fill the gap in the clutter theory and thus allow the completion of the GEO SAR System Performance Assessment Methodology [1, 2].

We presented a new physics-based clutter model for short vegetation landscape that is applicable to estimate GEO SAR performance, but is also suitable for a wide range of SAR systems.

This model needs to be completed but the first part, that is the estimation of the coherent power fraction, shows a reasonable consistency between the developed theory and the numerical simulations as shown in Fig. 5 and in Tab. 1.

Figure 6 shows the diagram of the process to build the clutter model. From the windspeed we get the wheat standard deviation and its uncertainty (using the two-line fit shown in Fig. 3). Then we use the Γ bell-shape function (Eq. 11) to compute the expected coherent power fraction. After this, we compute the incoherent power fraction using Eq. 4.

The last step to complete the wheat clutter model would be modelling the tails of the PDF. This model for short vegetation should be supplemented with models for trees and ocean, and then realistic landscapes can be simulated.

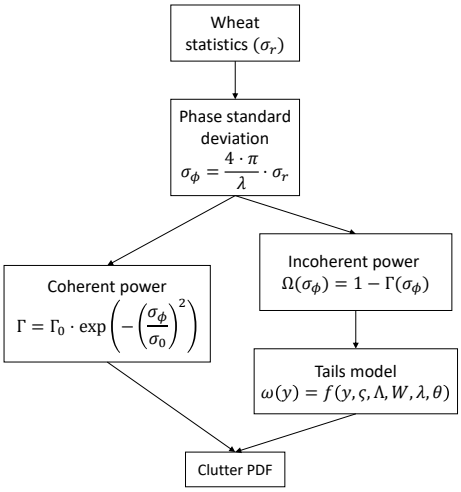

Fig. 6: Diagram of clutter modelling process.

6. REFERENCES

[1] S. Hobbs, C. Convenevole, A. M. Guarnieri, and G. Wadge, "Geostare system performance assessment methodology," in *International Geoscience and Remote Sensing Symposium (IGARSS)*, 2016, vol. 2016-November, pp. 1404–1407.

[2] C. Convenevole and S. Hobbs, "Methodology for estimating clutter limited geosynchronous synthetic aperture radar performance," in *IET International Radar Conference (Radar2019), in proceedings*, 2019.

[3] P. Lombardo and J. B. Billingsley, "New model for the doppler spectrum of windblown radar ground clutter," *IEEE National Radar Conference - Proceedings*, pp. 142–147, 1999.

[4] J. B. Billingsley, A. Farina, F. Gini, M. V. Greco, and L. Verrazzani, "Statistical analyses of measured radar ground clutter data," *IEEE Transactions on Aerospace and Electronic Systems*, vol. 35, no. 2, pp. 579–593, April 1999.

[5] J.B. Billingsley, *Low-angle Radar Land Clutter: Measurements and Empirical Models*, William Andrew Pub., 2002.

[6] S. Hobbs, C. Seynat, and P. Matakidis, "Videogrammetry: A practical method for measuring vegetation motion in wind demonstrated on wheat," *Agricultural and Forest Meteorology*, vol. 143, no. 3-4, pp. 242–251, 2007.

[7] S. Hobbs, "Database of individual wheat plant motion in wind: Application to radar imaging of vegetation," *Agricultural and Forest Meteorology*, vol. 148, no. 11, pp. 1860–1868, 2008.